Erratum

Werner syndrome protein participates in a complex with RAD51, RAD54, RAD54B and ATR in response to ICL-induced replication arrest

Marit Otterlei, Per Bruheim, Byungchan Ahn, Wendy Bussen, Parimal Karmakar, Kathy Baynton and Vilhelm A. Bohr

Journal of Cell Science 119, 5215 (2006) doi:10.1242/jcs.03359

There was an error in the first e-press version of the article published in *J. Cell Sci.* **119**, 5137-5146.

The first e-press version of this article gave the page range as 5114-5123, whereas it should have been 5137-5146.

We apologise for this mistake.

Werner syndrome protein participates in a complex with RAD51, RAD54, RAD54B and ATR in response to ICL-induced replication arrest

Marit Otterlei[1,2,*], Per Bruheim[1,3,§], Byungchan Ahn[1,4,§], Wendy Bussen[5], Parimal Karmakar[1,6], Kathy Baynton[7] and Vilhelm A. Bohr[1]

[1]Laboratory of Molecular Gerontology, National Institute on Aging, NIH, 5600 Nathan Shock Dr., Baltimore, MD 21224, USA
[2]Department of Cancer Research and Molecular Medicine, Laboratory Centre, Faculty of Medicine, Norwegian University of Science and Technology, Erling Skjalgsons gt. 1, N-7006 Trondheim, Norway
[3]Department of Biotechnology, Norwegian University of Science and Technology, N-7491 Trondheim, Norway
[4]Department of Life Sciences, University of Ulsan, Ulsan 680-749, Korea
[5]Department of Molecular Biophysics and Biochemistry, Yale University School of Medicine, 333 Cedar St, SHM-C130, New Haven, CT 06515, USA
[6]Department of Life Science and Biotechnology, Jadavpur University, Kolkata-700 032, WB, India
[7]Research Center, Ste. Justine's Hospital, 3175 Cote Ste. Catherine, Montreal, Quebec H3T 1C5, Canada

*Author for correspondence (e-mail: marit.otterlei@ntnu.no)
§These authors contributed equally to this work

Accepted 5 October 2006
Journal of Cell Science 119, 5137-5146 Published by The Company of Biologists 2006
doi:10.1242/jcs.03291

Summary

Werner syndrome (WS) is a rare genetic disorder characterized by genomic instability caused by defects in the *WRN* gene encoding a member of the human RecQ helicase family. RecQ helicases are involved in several DNA metabolic pathways including homologous recombination (HR) processes during repair of stalled replication forks. Following introduction of interstrand DNA crosslinks (ICL), WRN relocated from nucleoli to arrested replication forks in the nucleoplasm where it interacted with the HR protein RAD52. In this study, we use fluorescence resonance energy transfer (FRET) and immune-precipitation experiments to demonstrate that WRN participates in a multiprotein complex including RAD51, RAD54, RAD54B and ATR in cells where replication has been arrested by ICL. We verify the WRN-RAD51 and WRN-RAD54B direct interaction in vitro. Our data support a role for WRN also in the recombination step of ICL repair.

Key words: WRN, ICL, RAD51, RAD54B, ATR, DNA repair

Introduction

Individuals with Werner syndrome (WS) are afflicted with a genomic instability disorder derived from defects in the *WRN* gene encoding a member of the RecQ DNA helicase family (Martin, 1978; Yu et al., 1996). RecQ helicases are highly conserved from bacteria to human; however, bacteria possess a single RecQ enzyme, whereas in humans, five RecQ members have been identified so far (Hickson, 2003). Deficiencies in three of the human RecQ helicases, WRN (Martin et al., 1970), BLM and RECQL4, are responsible for Werner syndrome (WS), Bloom syndrome (BS), and Rothmund-Thomson syndrome (RTS), respectively. All three disorders are characterized by decreased genomic stability leading to increased cancer incidence (Hickson, 2003). WS is further classified as a segmental progeroid syndrome since patients display the early onset of many age-associated pathologies, such as arteriosclerosis, cataracts, diabetes mellitus type II, greying and loss of the hair, wrinkling of the skin, osteoporosis and increased predisposition to cancer development, primarily of mesenchymal origin (Hickson, 2003; Opresko et al., 2003). Cells from WS patients display marked chromosomal rearrangements and deletions (Fukuchi et al., 1989; Grigorova et al., 2000; Salk, 1982) and a shortened life span in culture (Martin et al., 1970). The molecular basis of the premature senescence and the genomic instability in WS cultured cells is not yet clear.

The RecQ helicases display 3′ to 5′ unwinding directionality on DNA on a variety of structures including recombination intermediates such as Holliday junctions (HJ) (Constantinou et al., 2000). The WRN protein is unique among human RecQ helicases in that it also contains a 3′ to 5′ exonuclease activity (Huang et al., 1998). How the WRN helicase and exonuclease function to resolve DNA structures in vivo is currently unclear; however, cooperativity between the two activities has been suggested to occur in some situations (Opresko et al., 2003; Opresko et al., 2001; Opresko et al., 2004).

WRN interacts physically and functionally with a number of proteins involved in different DNA metabolic pathways including replication protein A (RPA) (Brosh et al., 1999), proliferating cell nuclear antigen (PCNA) (Lebel et al., 1999), polymerase δ (Kamath-Loeb et al., 2000), flap endonuclease 1 (FEN-1) (Brosh et al., 2001), RAD52 (Baynton et al., 2003), the MRN complex through binding to NBS1 (Cheng et al., 2004), the Ku heterodimer (Cooper et al., 2000; Hsu et al., 2000), and TRF2 (Opresko et al., 2002). Thus, WRN may be a multi-tasking enzyme that functions in several genome maintenance pathways, possibly by co-ordinating their progression.

One process in which WRN function has been strongly implicated is the recovery of arrested replication forks (Baynton et al., 2003; Sakamoto et al., 2001). Replication fork

arrest and collapse may lead to double-strand breaks (DSB) that are repaired in mammalian cells by either non homologous end joining (NHEJ) or homologous recombination (HR) (for reviews, see Lieber et al., 2003; West, 2003). The essentially error-free HR repair pathway is currently viewed as the major mechanism for re-establishing stalled replication forks during S-phase in human somatic cells. The current model for the repair and restart of an arrested replication fork involves a structure called a 'half chicken foot' or a 'chicken foot' resembling a Holliday junction that can be resolved by recombination (reviewed in Helleday, 2003). Studies in *Escherichia coli* indicate that the 'chicken foot' can be processed by the DNA helicase activity of RecQ together with the 5′ to 3′ exonuclease function of RecJ prior to replication restart (Courcelle et al., 2003). Interestingly, recent data have shown that WRN helicase unwinds the chicken-foot intermediate and stimulates FEN-1 to cleave the unwound product in a structure-dependent manner (Sharma et al., 2004). However, the precise steps and proteins involved in this process are still unclear (reviewed in Helleday, 2003; Hickson, 2003; West, 2003) and under intense investigation.

RecQ helicases and RAD HR proteins have also been documented to collaborate in DNA maintenance pathways distinct from stalled replication fork recovery. The *Saccharomyces cerevisiae* RecQ helicase homolog, Sgs1p, functions together with *RAD52* epistasis group members in a telomerase-independent alternative lengthening of telomeres (ALT) pathway (Le et al., 1999; Teng and Zakian, 1999). ALT pathways have also been detected in a number of immortalized human cell lines lacking telomerase (Bryan et al., 1997; Colgin and Reddel, 1999), and ALT cells contain ALT-associated PML bodies consisting of promyelocytic leukaemia protein (PML), telomeric DNA, the telomere binding proteins TRF1 and TRF2, the RAD homologous recombination (RAD-HR) proteins RAD50, RAD51, RAD52, MRE11, NBS1, ATR, and the BLM and WRN helicases (Barr et al., 2003; Henson et al., 2002). *WRN* mutations have been associated with increased telomere dysfunction in cells cultured from later generation mice lacking the telomerase RNA component, *Terc* (Chang et al., 2004). These mice elicit classic WS-like premature aging manifested by precocious death, graying of the hair, osteoporosis, type II diabetes and cataracts. These data support a role for WRN, together with some of the RAD HR proteins, in a recombination-dependent ALT pathway.

ICL repair is poorly understood in mammalian cells, but is thought to involve a combination of nucleotide excision repair (NER), translesion synthesis (TLS) and/or recombination (De Silva et al., 2000; Zheng et al., 2003). ICLs are probably not repaired until they are encountered by a DNA replication fork (Akkari et al., 2000). Cells cultured from patients afflicted with WS, BS and Nijmegen breakage syndrome (deficient for the NBS1 protein) all exhibit elevated sensitivity to ICLs (Pichierri and Rosselli, 2004; Rosselli et al., 2003). Indeed, WRN was recently shown to relocate to sites of arrested replication induced by ICLs, where it physically and functionally interacts with RAD52. Furthermore, WRN was found to stimulate RAD52-mediated strand annealing and RAD52 enhance WRN helicase activity on specific substrates (Baynton et al., 2003). Interestingly, RAD52 was shown to interact physically and functionally with the XPF/ERCC1 DNA structure-specific endonuclease involved in ICL repair (Motycka et al., 2004), and WRN was recently found to be required for ICL repair in an in vitro assay and thus suggested to be a candidate helicase involved in the early steps in processing ICL (Zhang et al., 2005). In the early pre-synapsis step of HR, a single-stranded DNA (ssDNA) tail is converted to a nucleoprotein filament consisting of RPA, RAD51, RAD52, RAD54 and possibly RAD54B (Alexeev et al., 2003; Tan et al., 2003; Tanaka et al., 2000). The formation of WRN and RAD52 complexes at arrested replication forks induced by ICL, together with the observed stimulation of RAD52 strand annealing activity by WRN in vitro, suggests that WRN may function both during early steps of processing ICL (Zhang et al., 2005; Zhang et al., 2003) and during pre-synapsis in later steps of ICL repair. To evaluate further the potential role of WRN in ICL repair/recovery processes, we examined whether WRN interacts with other members of the RAD52 epistasis group following replication arrest. We report here that WRN re-localizes to a complex (or complexes) composed of RAD54, RAD51, RAD54B and ATR in response to replication arrest induced by treatment of cells with MMC. In vitro biochemical analyzes reveal that WRN associates directly with RAD51 and RAD54B. Based on our data we suggest a role for WRN in the resolution of stalled replication forks arrested by ICL, both as the candidate helicase during the early steps of processing ICL as suggested by Zhang et al. (Zhang et al., 2005) and during the later pre-synapsis step of homologous recombination.

Results

Nuclear localization dynamics of WRN, RAD51, RAD54 and RAD54B in untreated cells

Previous fluorescence resonance energy transfer (FRET) data demonstrated that prolonged exposure (16-24 hours) of HeLa cells to MMC leads to the re-localization of RAD52 and WRN to sites of arrested replication where they physically interact (Baynton et al., 2003). To study intracellular localization and re-localization dynamics as well as to identify potential protein-protein interactions between WRN and other HR components upon replication fork blockage using fluorescence microscopy and FRET analysis, we cloned human RAD51, RAD54 and RAD54B proteins as C-terminal fusions to ECFP and EYFP.

Fig. 1 shows the nuclear localization of ECFP- and EYFP-tagged RAD51, RAD54 and RAD54B in live, untreated, cycling HeLa cells 16-24 hours after co-transfection. ECFP-RAD51 exhibited both punctuated and rod-shaped fluorescence patterns (Fig. 1, pictures 1 and 4), while WRN localized mainly in nucleoli as previously reported for endogenous WRN and both transient and stable expressing GFP-tagged WRN (Fig. 1, picture 2) (Baynton et al., 2003; Opresko et al., 2004; von Kobbe and Bohr, 2002). We tried to generate stable cell lines that constitutively expressed low (physiological) levels of ECFP-RAD51; however, after five weeks in selective medium, only 0.5% of the cells resistant to the selective antibiotic (geneticin) expressed ECFP-RAD51 (Fig. 1, picture 1, insert). However, the localization pattern of ECFP-RAD51 in the cells stably expressing ECFP-RAD51 was similar as in transiently transfected cells, and we therefore chose to use transiently transfected cells expressing medium to low levels of ECFP-RAD51 in our studies. As RAD51 has been reported to form S-phase specific nuclear foci (Tarsounas et al., 2003; Tashiro et al., 1996), we co-transfected ECFP-RAD51 with EGFP-PCNA to determine if these foci were replication

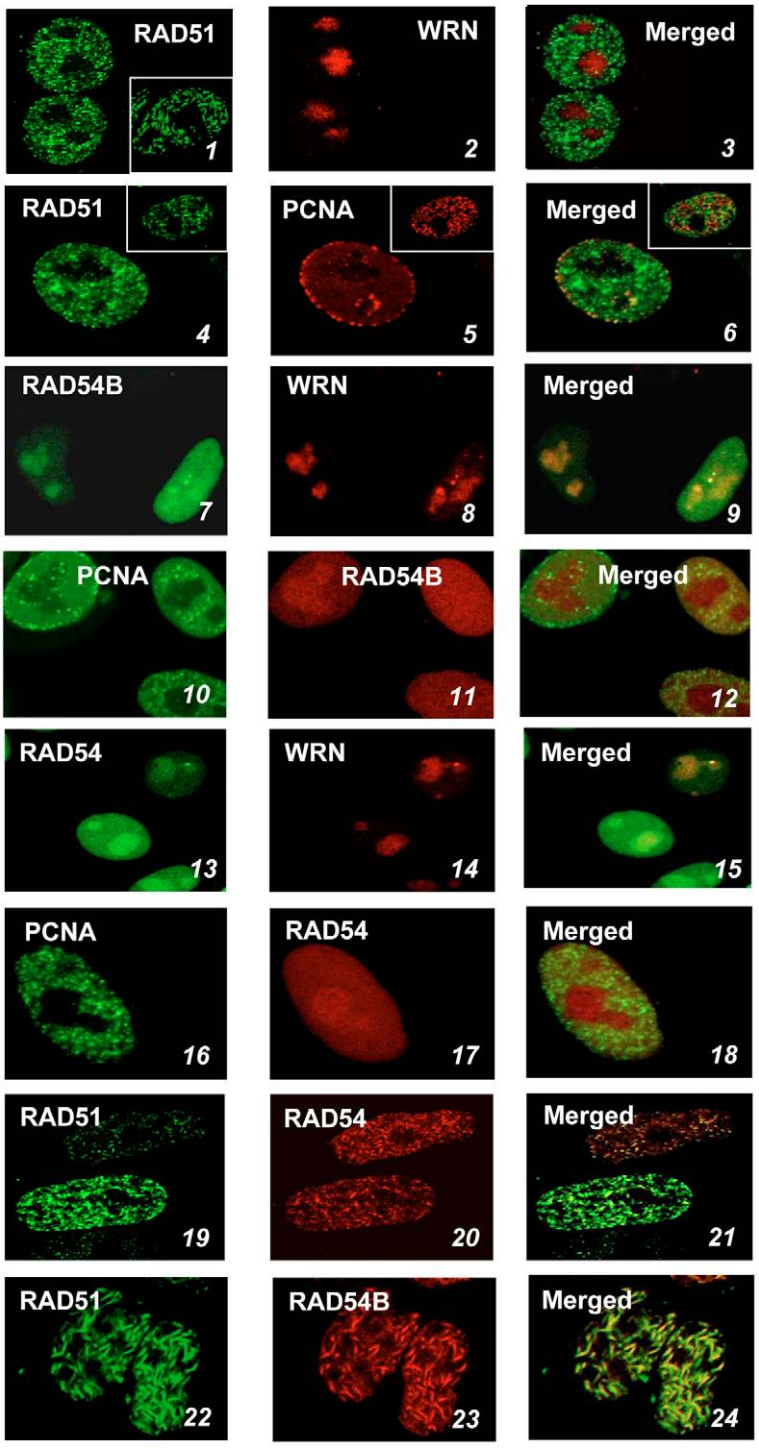

Fig. 1. Subcellular localization of WRN-, RAD51-, RAD54-, RAD54B- and PCNA-ECFP and EYFP constructs in live cycling HeLa cells. Cells co-transfected with: pictures 1-3*:* ECFP-RAD51 and EYFP-WRN. Inset picture 1: a stable ECFP-RAD51 expressing cell after 5 weeks in cell culture; pictures 4-6*:* ECFP-RAD51 and EYFP-PCNA; pictures 7-9: ECFP-RAD54B and EYFP-WRN; pictures 10-12: ECFP-PCNA and EYFP-RAD54B; pictures 13-15: ECFP-RAD54 and EYFP-WRN; pictures 16-18: ECFP-PCNA and EYFP-RAD54; pictures 19-21: ECFP-RAD51 and EYFP-RAD54; pictures 22-24: ECFP-RAD51 and EYFP-RAD54B.

forks. Tagged PCNA forms distinct foci in S phase cells that co-localize completely with endogenous PCNA at sites of bromo-deoxyuridine (BrdU) incorporation thereby representing sites of DNA synthesis (Leonhardt et al., 2000). Fig. 1 (pictures 4-6) shows that some of the RAD51 foci co-localize with PCNA in nuclear foci in unsynchronized cultures, but that there were additional RAD51 foci not co-localizing with PCNA. Cells over-expressing RAD51 have been reported to exhibit elevated levels of RAD51 foci, faster repair rates of etoposide-induced DSBs, higher levels of spontaneous HR and apoptosis, and reduced long-track HR in the *hprt* gene (Lundin et al., 2003). However, importantly for the present work, increased foci formation due to over-expression of the ECFP-RAD51 fusion protein did not affect the intracellular localization of either co-transfected WRN or PCNA (Fig. 1, pictures 2 and 5, respectively), indicating that over-expression of RAD51 did not itself induce replication arrest.

Cells transfected with ECFP-RAD54B alone demonstrated diffuse nucleoplasmic localization with some minor accumulation in the nucleoli where it co-localized with co-transfected EYFP-WRN (Fig. 1, pictures 7 and 8). RAD54B and WRN also co-localized in some nucleoplasmic spots that may represent PML bodies or replication foci arrested by endogenous damage. ECFP-RAD54B did not co-localize with PCNA in replication foci (Fig. 1, pictures 10-12). When co-transfected, RAD54 and WRN co-localized in nucleoli similar to RAD54B and WRN (Fig. 1, pictures 13-15), furthermore no co-localization was seen between RAD54 and PCNA (Fig. 1, pictures 16–18).

Human RAD54 and RAD54B belong to the SNF2/SW12 family of DNA-dependent ATP-ases (Swagemakers et al., 1998; Tanaka et al., 2000) and experiments suggest that yeast Rad54 plays an active role in pre-synapsis by stabilizing the Rad51 single-strand DNA filament (Mazin et al., 2003). Human RAD54 and RAD54B bind to RAD51 in vitro (Golub et al., 1997; Wesoly et al., 2006) and the proteins are associated in the same complex in vivo (Tanaka et al., 2000). To examine whether the tagged RAD51, RAD54 and RAD54B proteins were functional with regard to protein-protein interactions, we co-transfected EYFP-RAD54 and EYFP-RAD54B with ECFP-RAD51. RAD54 completely re-localized into a rod-shaped fluorescent pattern also observed in cells expressing RAD51 alone (Fig. 1, pictures 19–21 compared to pictures 1 and 4), suggesting that the two proteins bind directly to each other in vivo concurring with previous work (Golub et al., 1997). Similar to RAD54, RAD54B re-localized into the rod-shaped RAD51 pattern when co-transfected with RAD51 (Fig. 1, pictures 22-24) in accordance with participation in the same complex (Tanaka et al., 2002). Rad54 is reported to increase protection of DNA in a Rad51 double-stranded (ds) DNA filament from restriction enzyme digestion (Mazin et al., 2003); thus, the rod-shaped pattern of ECFP-RAD51 might be dsDNA-ECFP-RAD51 filaments that recruit both RAD54 and RAD54B.

Co-localization of RAD51, RAD54 and RAD54B with WRN at the vicinity of replication centers after MMC induced lesions

To determine the appropriate mitomycin (MMC) concentration that introduces DNA damage at levels leading to replication arrest and yet is minimally cytotoxic, survival and proliferation of HeLa cells were tested over four days following 16 hours of exposure to 0.2 and 0.5 μg ml^{-1} MMC. As shown in Fig. 2A, the high percentage of live cells on day 1 combined with an increase in the culture optical density

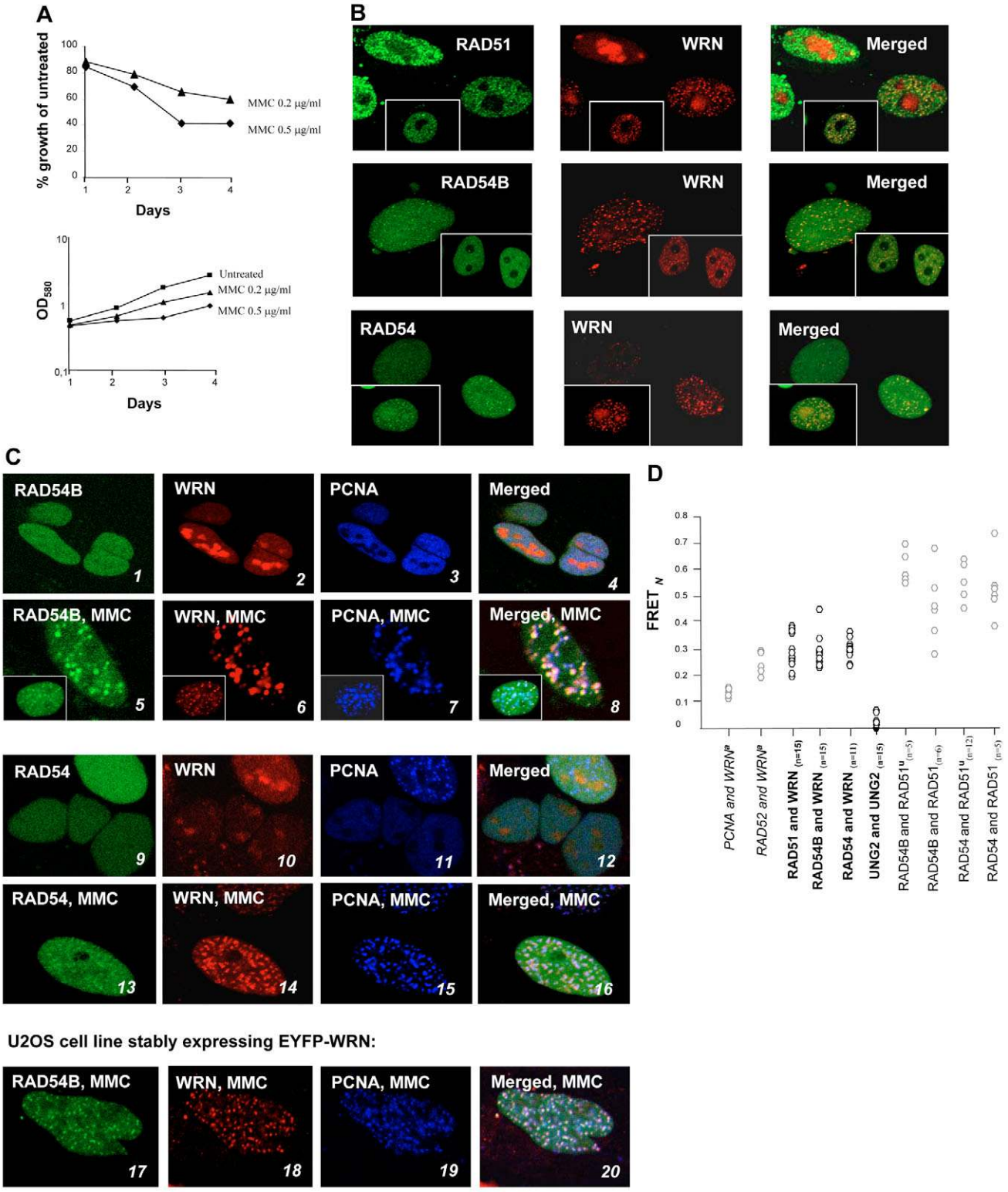

Fig. 2. See next page for legend.

from days 1 to 3 demonstrated low cytotoxicity of both MMC dosages (Fig. 2A). MMC concentration of 0.5 μg ml^{-1} clearly introduced important levels of replication blocking lesions as manifested by the 3 day proliferative arrest observed in the treated cells followed by the recovery to growth rates that were comparable to untreated cell cultures at day 3 (Fig. 2A, lower graph), thus this dose was chosen for further studies.

Following treatment with 0.5 μg ml^{-1} MMC for 16-24 hours, we looked at localization patterns of the RAD proteins relative to WRN in transiently transfected HeLa cell cultures. Fig. 2B shows that the introduction of DNA intrastrand crosslinks with MMC treatment caused RAD51 (upper row), RAD54B (mid row) and RAD54 (lower row) to co-localize with WRN to discrete nucleoplasmic foci. Previously, WRN and RAD52 were shown to co-localize and interact at spots resembling arrested replication forks in identically treated cells (Baynton et al., 2003). At the top of upper row Fig. 2B, one cell expressing higher levels of both RAD51 and WRN than the other cells in the image, but with no co-localization between the two proteins is shown. This cell, which likely represents a cell that is not arrested in S-phase, reflects that not all cells have achieved identical load of DNA damages after treatment of MMC for 24 hours and furthermore that RAD51 over-expression with rod-shaped fluorescence by itself does not lead to co-localization with WRN.

To verify that the co-localizing spots containing WRN and the RAD-proteins are in the vicinity of 'arrested' replicating centers, we co-transfected HeLa cells with ECFP-RAD54 or ECFP-RAD54B, with EYFP-WRN and HcRed-PCNA. Fig. 2C, shows that RAD54B (pictures 1-8), RAD54 (pictures 9-16), WRN and PCNA do co-localize in foci after MMC treatment in co-transfected HeLa cells, but not in untreated cells. In a stable EYFP-WRN expressing ALT (alternative lengthening of telomeres) cell line (U2OS) expressing 5-6-fold more EYFP-WRN than endogenous WRN (data not shown), we previously observed that WRN co-localized with PCNA in 28-58% of the replication foci (Opresko et al., 2004). The level of EYFP-WRN in this cell line is similar to the transient transfected HeLa cells used in this study as determined by fluorescence intensities. Fig. 2C, pictures 17-20, show that similar to in the treated HeLa cells nearly 100% of the RAD54B spots co-localized with WRN and PCNA after MMC treatment in the stable EYFP-WRN expressing cells, supporting that WRN and RAD54B re-localized to the vicinity of replication forks upon replication arrest.

Fluorescence resonance energy transfer (FRET)

Due to the resolution limits of fluorescence microscopy, proteins that co-localize may not in fact interact or be in the same complex (directly or indirectly). Therefore, we used fluorescence resonance energy transfer (FRET) to determine whether the fluorescently tagged RAD proteins and WRN were in the same complex [i.e. less than 100 Å (10 nm) apart] after cellular exposure to MMC. Positive FRET is detected if the intensity of emitted light from the acceptor fluorochrome (EYFP) after excitation of the donor fluorochrome (ECFP) is greater than the light emitted from cells transfected with ECFP or EYFP tagged proteins alone (i.e. background levels). FRET values within punctuated foci obtained from experiments identical to those described and shown in Fig. 2B, normalized against protein expression levels ($FRET_N$), are presented as a dot plot in Fig. 2D. Variations in $FRET_N$ in different regions of interest (ROI) are expected since they measure the dynamic events in many replication sites/forks within the vicinity of replication centers simultaneously. Our results indicate that WRN interacts directly or is very closely associated in either a single multiprotein complex or in independent subcomplexes with RAD51, RAD54 and RAD54B. The $FRET_N$ values obtained for WRN-RAD51, WRN-RAD54 and WRN-RAD54B are higher on average than those determined for two previously published WRN interactions: WRN-RAD52 (just slightly higher); and WRN-PCNA (at least twofold greater) (Baynton et al., 2003). ECFP- and EYFP-tagged UNG2 proteins were used as a negative FRET control since UNG2 is a monomer that localizes to replication foci (Otterlei et al., 1999). UNG2-ECFP and UNG2-EYFP exhibited essentially 100% co-localization while the $FRET_N$ values using these instrument settings were less than zero in more than 95% of the UNG2 expressing cells. In the remaining <5% cells, $FRET_N$ values were greater than zero but still fourfold lower than values determined for WRN and RAD51, WRN and RAD54 and WRN and RAD54B (Fig. 2D).

FRET was also used to examine functionality of the tagged fusion proteins with regard to protein-protein interactions. FRET was examined after co-transfection of ECFP-RAD51 and EYFP-RAD54, and ECFP-RAD51 and EYFP-RAD54B, which lead to re-localization of RAD54 and RAD54B into a

Fig. 2. (A) Survival and growth of HeLa cells treated with MMC. Data from untreated cells and cells exposed to MMC (0.5 and 0.2 μg ml^{-1}) for 16 hours are shown. Each point represents six parallel wells. Error bars are undetectable as they are smaller than the symbols. (B) Co-localization of WRN with RAD51, RAD54B and RAD54 after treatment with MMC. Co-localization of ECFP-RAD51 and EYFP-WRN (upper row), ECFP-RAD54B and EYFP-WRN (middle row), ECFP-RAD54 and EYFP-WRN (lower row) in HeLa cells treated with MMC (0.5 μg ml^{-1}) over night. (C) Re-localization of WRN, RAD54 and RAD54B to PCNA foci after MMC treatment. HeLa (pictures 1-16) and U2OS cells (pictures 17-20) were treated with MMC (0.5 μg ml^{-1}) over night to arrest the cells in S-phase. HeLa cells co-transfected with ECFP-RAD54B, EYFP-WRN, HcRed-PCNA: untreated (pictures 1-4) and treated with MMC (pictures 5-8). HeLa cells co-transfected with ECFP-RAD54, EYFP-WRN, HcRed-PCNA: untreated (pictures 9-12) and treated with MMC (pictures 13-16). Stable EYFP-WRN expressing U2OS cells co-transfected with ECFP-RAD54B and HcRed-PCNA and treated with MMC (pictures 17-20). (D) $FRET_N$ values between WRN and the RAD52 epistasis proteins after MMC treatment over night, and between RAD51-RAD54 and RAD51-RAD54B. [a]Represents previously published data (Baynton et al., 2003) that was taken using the same conditions and settings as the current experiments. It is presented here for comparative purposes. [U]untreated cells. $FRET_N$ [$FRET_N$=FRET/$(I_1 \times I_3)^{1/2}$] represents FRET normalized against protein expression levels measured from intensities (I) (given as arbitrary units below 250). FRET is calculated from the mean of intensities within a region of interest containing more than 25 pixels. Within the region of interest, all pixels had intensities below 250, and the I levels were between 85-190 for the donor (ECFP) and between 55-155 (EYFP) for the acceptor, respectively. Corresponding pictures from which the data were derived are shown in Fig. 2B and Fig. 1, pictures 19-24 (*RAD54-RAD51*^{U} and *RAD54B–RAD51*^{U}). The background level outside foci, i.e. the co-localizing area, is 0, which is also the FRET value determined for more than 95% of foci with co-localizing UNG2-ECFP and UNG2-EYFP proteins.

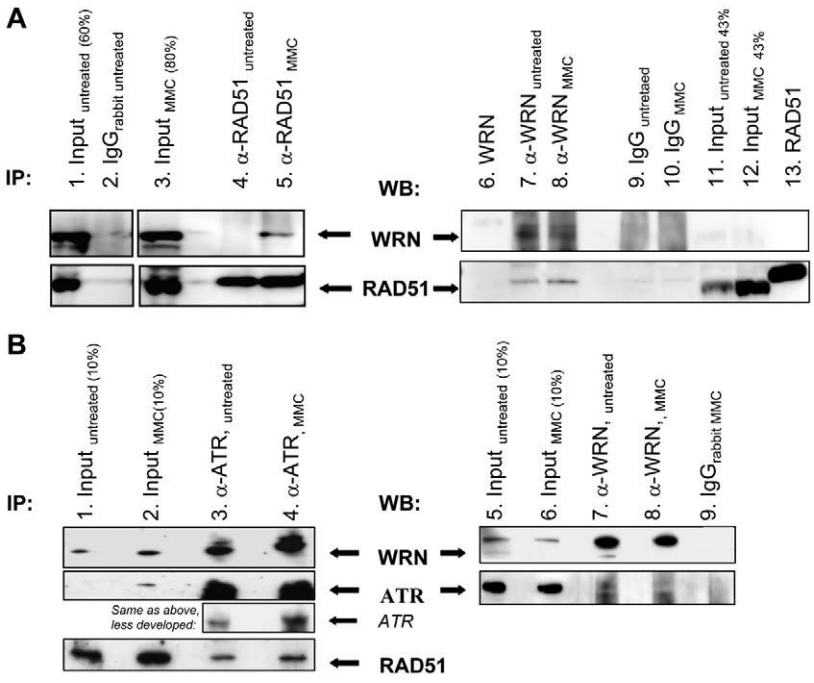

Fig. 3. Co-immunoprecipitation of WRN, RAD51 and ATR. (A) WRN is pulled down with RAD51 (H-92) from whole cell extracts prepared from HeLa cells treated with MMC (0.5 μg ml^{-1}), lane 5. In a WRN pulled down with the rabbit polyclonal anti-WRN (ab17987) we co-immunoprecipitated RAD51, lanes 7 and 8. Mouse anti-WRN (BD) or polyclonal anti-WRN (ab17987) and anti-RAD51 (ab1837) were used for the WBs. (B) WRN is pulled down with ATR from whole cell extracts prepared from HeLa cells. Rabbit polyclonal anti-ATR (ab91) and anti-WRN (ab200) were used for IP, and monoclonal mouse anti-WRN (BD) and anti-ATR (ab91) were use for WB. Input represents whole cell lysate. IgG is normal rabbit IgG (SC).

rod-shaped fluorescence pattern (Fig. 1, pictures 19-24). The calculated $FRET_N$ values further indicate that RAD51 binds directly to both RAD54 and RAD54B proteins in vivo (Fig. 2D). Furthermore, these $FRET_N$ values were higher than those determined for WRN-RAD51, WRN-RAD52, WRN-RAD54 and WRN-RAD54B, which is expected since co-expression with RAD51 completely relocates RAD54 and RAD54B. Thus, a large fraction of the tagged molecules present within a given ROI on the filaments are likely to interact, while fewer of the tagged WRN and RAD proteins present in a particular ROI around foci may participate in the WRN-RAD interactions. This implies that the interactions between WRN and the RAD51, 54 and 54B proteins at arrested replication sites are more dynamic than the RAD51-RAD54B and RAD51-RAD54 interactions.

Formation of a multiprotein complex containing WRN, RAD51 and ATR in response to MMC treatment

To confirm that WRN, RAD51, RAD54 and RAD54B are in the same complex formed at blocked replication forks, we performed co-immunoprecipitation (co-IP) experiments. Since the proteins assemble together at arrested replication sites, these complexes are expected to associate with chromatin. To access most protein complexes within the cells, also chromatin bound complexes, we performed immunoprecipitation experiments of endogenous proteins in sonicated whole cell extracts digested with DNAse. Using this approach we could IP WRN with RAD51 using anti-RAD51 antibody in cell extracts prepared from MMC treated cells, but not, or far less, from untreated cells (Fig. 3A, lanes 4 and 5). The reciprocal experiment using anti-WRN antibodies could co-IP RAD51 in extracts from both treated and untreated cells (Fig. 3A, lanes 7 and 8). We did not have sufficiently specific and/or sensitive RAD54 and RAD54B antibodies to examine co-IP WRN of with the endogenous RAD54 and RAD54B proteins.

The ATR kinase is primarily responsible for eliciting the S-phase response to replication blocks. Furthermore, WRN is phosphorylated in an ATM/ATR-dependent manner and co-localizes with ATR in nuclear foci after ICL induction (Pichierri and Rosselli, 2004; Pichierri et al., 2003). Therefore, we wanted to examine whether WRN complexed with ATR in MMC treated cells by an immunoprecipitation approach. We were able to pull down, using two different ATR antibodies, what appears to be increasing amounts WRN from cell lysates prepared from MMC treated cells (Fig. 3B, lanes 3 and 4, and data not shown). We also detected RAD51 with immunoprecipitated ATR (Fig. 3B, lanes 3 and 4). The reciprocal co-IP of ATR and WRN could not easily be evaluated due to low specificity of both of the antibodies (Fig. 3B, lanes 7 and 8).

Thus, although the results for RAD54 and RAD54B co-IPs were inconclusive, we nevertheless found that WRN interacts with RAD51 and ATR, either directly or indirectly through another as yet unidentified protein. Furthermore, this WRN-RAD51-ATR complex forms in response to replication forks blocked by DNA ICLs.

WRN interacts with both RAD51 and RAD54B proteins in vitro

Enzyme-linked immunosorbent assays (ELISAs) using purified recombinant proteins were undertaken to further characterize the interactions detected between WRN and the RAD HR proteins. RAD52 was used as a positive control as it has been shown previously to interact with both WRN (Baynton et al., 2003) and RAD51 (Shen et al., 1996). Fig. 4A demonstrates that WRN and RAD51 interacted regardless of which protein was used to coat the wells. The association, determined by the absorbance at 490 nm, between RAD51 and WRN was comparable to that observed between RAD51 and RAD52, but lower than that detected between WRN and RAD52 (Fig. 4A).

Results from ELISAs examining RAD54 and RAD54B interactions with WRN (coat) are shown in Fig. 4B. RAD54B bound detectably to WRN while an association between RAD54 and WRN was barely observable over background. The binding of RAD54B to WRN was less pronounced than RAD52, but stronger than RAD51.

Dot blot assays, in which the indicated proteins immobilized to PVDF membranes were incubated in a solution either with or without (negative control) WRN and subsequently probed with an anti-WRN antibody, were performed to corroborate

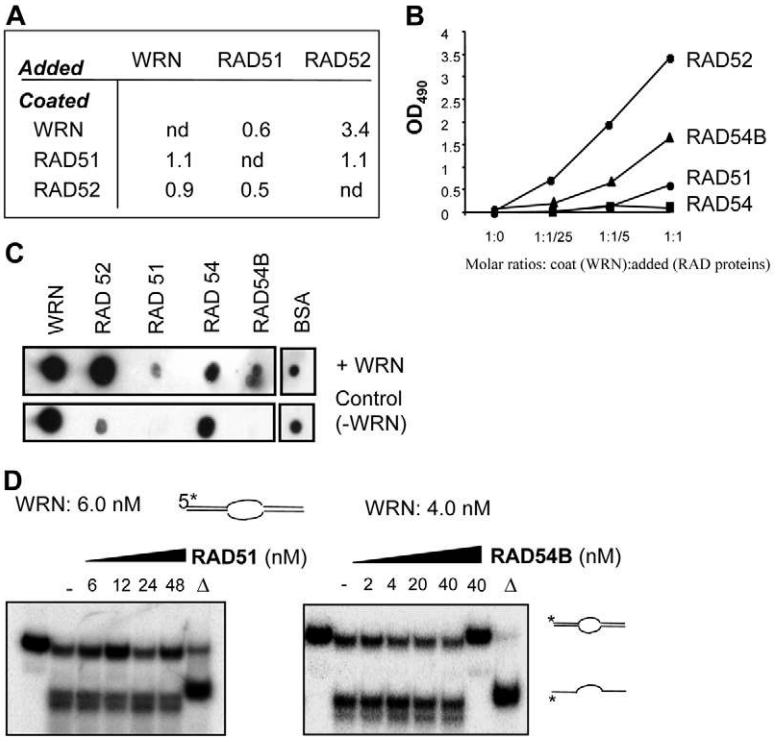

Fig. 4. WRN binds directly to RAD51 and RAD54B. (A) Reciprocal ELISAs showing direct binding between RAD51 and WRN. WRN, RAD52 (positive control), BSA (negative) and RAD51 were coated on microtiter plates. Binding of WRN, RAD52 and RAD51 to each other were measured as described in Materials and Methods. Values (OD_{490nm}) for 1:1 molar ratio between the proteins are given. (B) Relative binding of RAD54B, RAD54, RAD51 and RAD52 to WRN coat in ELISA. Both results (A and B) are representative of one out of at least three independent experiments. Absorbance (OD_{490nm}) is given as mean of duplicates adjusted for background binding to BSA in parallel duplicate wells. (C) Dot blot assay demonstrating a direct interaction between WRN and RAD51, and WRN and RAD54B. PVDF membranes with immobilized proteins were incubated in milk-solutions with or without WRN, and analyzed for WRN binding. (D) RAD51 and RAD54B do not modulate WRN helicase activity on a 12 bp bubble substrate. Native gels showing WRN (6.0 nM and 4.0 nM) mediated unwinding of a 12 bp 5′-labeled bubble substrate after adding increasing amounts of RAD51 (6, 12, 24 and 48 nM) and RAD54B (2, 4, 20 and 40 nM).

ELISA results. A strong interaction was detected between WRN and RAD52, positive binding was observed to RAD54B and a weak but positive association was detected between WRN and RAD51 (Fig. 4C). However, a WRN-RAD54 interaction could not be evaluated due to non-specific binding of the WRN antibodies to RAD54, similar to that seen with the negative control, BSA.

The in vitro binding data demonstrate that WRN binds directly to both RAD51 and RAD54B, in agreement with FRET observations. However, even though the FRET results indicate that WRN and RAD54 are as close as RAD54B and RAD51, and therefore, directly interact, we detected a weaker association between purified RAD54 and WRN proteins in ELISA. The discrepancy between the in vivo and in vitro data may be attributable to the lack of specific post-translational modifications or a mediator protein in the in vitro system that is necessary for the interaction to occur.

We find that co-transfection and over-expression of WRN and RAD51 does not lead to co-localization of the two proteins unless the cells are treated with DNA damaging agent such as MMC on the contrary to what is seen for RAD54-RAD51 and RAD54B-RAD51 (Fig. 1, pictures 19-24). At the same time WRN and RAD51 seem to interact in vitro in ELISA and Dot blot assay. An explanation for this may be that WRN need some sort of post-translational modifications, such as phosphorylation, to interact with RAD51 and that WRN isolated from insect cell cultures are sufficiently phosphorylated to mediate such interaction also in vitro.

RAD51 and RAD54B do not modulate WRN activity on fork or bubble substrates

Several of the reported physical interactions between WRN and its various protein partners modify WRN activity on defined substrates. Previously, we found that RAD52 stimulated WRN helicase activity on a 12 bp bubble substrate and inhibited WRN exonuclease activity (Baynton et al., 2003). Using substrates representing replication fork/recombination intermediates (bubble or fork substrates), no significant modulation of either helicase or exonuclease activity was observed in the presence of RAD51 or RAD54B (Fig. 4D and data not shown). Furthermore, no modulation of helicase activity was observed on a 3′-labeled (ddATP) bubble substrate, in which the exonuclease function is physically inhibited, upon the addition of RAD51 or RAD54B to assay mixtures (data not shown). Thus, under these assay conditions, RAD51 and RAD54B do not affect WRN helicase or exonuclease activities.

Discussion

We report here that WRN forms either a large single multiprotein complex or several dynamic subcomplexes involving RAD51, ATR, RAD54 and RAD54B at replication forks blocked by ICLs. WRN interacts directly with RAD51 and RAD54B; however, neither protein appears to modulate WRN's helicase or exonuclease activities on defined substrates in vitro. These results do not preclude the possibility that modulation could occur in vivo under conditions of appropriate substrate, post-translational modifications or, in the presence of an essential mediator protein. Together with previous studies showing that WRN interacts with RAD52 (Baynton et al., 2003), NBS1 in the MRN complex (Cheng et al., 2004) and Fen-1 (Brosh et al., 2001; Sharma et al., 2004), our results provide additional support of a role for WRN in recombination associated with replication restart.

Similar to WRN, BLM helicase also associates with RAD51 and ATR, and is phosphorylated by ATR (Davies et al., 2004; Wu et al., 2001). BS cells, like WS cell cultures, exhibit sensitivity to the DNA crosslinking agent mitomycin C (MMC) (Hook et al., 1984), suggesting that BLM also functions in ICL

repair. WRN and BLM co-localize in untreated cells and interact physically and functionally in vitro (von Kobbe et al., 2002). Thus, these two RecQ helicases may, in some instances, co-operate or provide back up functions in certain repair responses, including possibly ATR-mediated ICL repair. However, both helicases clearly execute non-overlapping, unique functions. Both BS and WS cell cultures exhibit increased crossover-associated recombination events and reduced recombination efficiency, but only BS cells specifically demonstrate elevated sister chromatid exchanges (SCEs) (Hickson, 2003).

Several lines of in vivo experimental evidence link WRN to stalled replication forks. For example, WRN relocates from nucleoli to nucleoplasmic foci after treatment with DNA damaging agents where it co-localizes with NBS1, RAD51 and RPA, respectively (Cheng et al., 2004; Sakamoto et al., 2001). Both WRN and NBS1 is phosphorylated in an ATR/ATM-dependent manner following replication arrest (Pichierri and Franchitto, 2004; Pichierri et al., 2003). Furthermore, NBS1 of the MRN assembly, in collaboration with FANCD2, participates in one of two parallel ATR controlled ICL induced pathways, the second pathway involving CHK1 (Pichierri and Rosselli, 2004). Co-operation between these two pathways leads to S phase checkpoint specific activation. Recent data strongly indicate that WRN and the MRN complex do act in a common pathway upon replication arrest (Franchitto and Pichierri, 2004). A model has been proposed describing how WRN and the MRN complex could co-operate in resolving abnormal structures at stalled replication forks during S-phase. Indeed, the interaction between NBS1 and WRN, combined with results from the current study demonstrating that WRN and ATR are present in the same complex in response to ICL induction, support a role for WRN in the NBS branch of the ATR controlled ICL repair response, possibly together with RAD51, RAD54, RAD54B and RAD52. RAD51 null mutation is embryonic lethal in mice while the cellular phenotypes of null RAD52 and RAD54 mutants in vertebrates are less severe, however they have been reported to have reduced HR frequency (both) and increased sensitivity to IR, the inter-strand cross-linking agent mitomycin C (MMC) and methyl methanesulfonate (MMS) (only RAD54–/–) (Essers et al., 1997; Rijkers et al., 1998).

Recent attempts to reconstitute psoralen ICL repair in vitro have revealed that PCNA is a stimulatory factor while RPA is essential at the incision step. Furthermore, RPA stimulates helicases, which in turn, create an open bubble region proximal to the ICL prior to incision (Zhang et al., 2003; Zhang et al., 2002). Candidate human helicases include WRN, BLM and RECQ1, all which bind to and are stimulated by RPA (Brosh et al., 2000; Brosh et al., 1999; Cui et al., 2004; Cui et al., 2003). In fact, recently WRN was found to interact with the pre-mRNA splicing Pso4-complex, and both WRN and the Pso4-complex were found to be required for ICL repair in an in vitro assay (Zhang et al., 2005). They propose a model where WRN is the candidate helicase involved in the early steps of processing ICL. Additional requirements for psoralen ICL repair include MutSβ, together with the ERCC1/XPF endonuclease, during initial lesion processing (Zhang et al., 2002). The endonuclease activity is essential for removing long non-homologous stretches from DNA 3′-OH ends during targeted homologous recombination and single strand annealing (SSA). XPF/ERCC1 also interacts physically and functionally with RAD52, resulting in the stimulation of the XPF/ERCC1 DNA structure-specific endonuclease function and inhibition of RAD52 strand annealing activity (Motycka et al., 2004). We previously demonstrated that RAD52 stimulates WRN helicase mediated unwinding of a bubble substrate and WRN enhances RAD52 strand annealing properties (Baynton et al., 2003). Thus, WRN may affect ICL repair at several levels by performing helix opening in co-operation with RPA and Pso4complex in accordance with the model suggested by Zhang et al. (Zhang et al., 2005; Zhang et al., 2003), prior to uncoupling of the ICL by XPF/ERCC1 endonuclease and strand annealing/invasion by the RAD HR proteins. Our data showing interactions of WRN with complexes containing ATR, RAD51, 52, 54 and 54B support a role for WRN also in the later HR steps of ICL-repair.

Materials and Methods

Purification of recombinant proteins

RAD52 and WRN were purified as described (Baynton et al., 2003; Opresko et al., 2002). RAD51 was a generous gift from Ian Hickson. Flag-RAD54 and RAD54B were prepared as described in Sigurdsson et al. (Sigurdsson et al., 2002) and Sehorn et al. (Sehorn et al., 2004), respectively.

Cloning of fusion proteins

Cloning of fluorescent-tagged expression constructs pEYFP-WRN, pECFP-RAD52, pECFP-PCNA, pUNG2-ECFP and pUNG2-EYFP has been previously described (Baynton et al., 2003; Aas et al., 2003). RAD51 was PCR amplified from pFB530 (Benson et al., 1994) and ligated into the *Pst*I/*Bam*HI restriction sites of pECFP-C1 vector (Clontech). RAD54 was PCR amplified from pBluescript (Sigurdsson et al., 2002) and cloned into the *Kpn*I site of pECFP-C1 and pEYFP-C1 vectors. RAD54B in pUC18 (Sehorn et al., 2004) was PCR amplified and cloned into the *Xho*I/*Xma*I site of pECFP-C1 and pEYFP-C1 vectors. All constructs were verified by sequencing. HcRed-PCNA and stable expressing EYFP-WRN U2OS cells have been previously described (Opresko et al., 2004).

Cell culture

Cells were transfected with the different constructs of fusion proteins using the calcium phosphate. method (Profection Promega) according to the manufacturer's recommendations. Stable ECFP-RAD51 expressing cells (HeLa) were cultured in DMEM media (Gibco) containing 10% fetal calf serum, gentamycin (100 μg ml^{-1}, Gibco), glutamine, fungizone and geneticin [G418, 400 μg ml^{-1} (Invitrogen), added 2 days after transfection]. For transient transfections the cells were examined after 16-24 hours, and no geneticin was added. Untransfected cells were cultured in the same media without geneticin.

Cell survival and growth in the presence of MMC

HeLa cells were seeded into four 96 well plates at three different cell densities. A dose response curve to MMC was determined for each cell concentration. All plates were incubated for 16 hours before being washed three times with PBS. At that time (day 1), the first plate was harvested using the MTT assay (Mosmann, 1983). Fresh medium was added to the remaining plates, which were further incubated for 1 to 3 days before being assayed for cell proliferation and survival by the MTT assay. The cell density permitting growth to be followed for four days without saturation of the OD_{570} signal after MTT addition in the control wells (no MMC added) were selected. The mean OD_{570} from 6 wells was used to calculate cells survival and plot the growth after addition of 0.5 μg ml^{-1} MMC.

Confocal microscopy and FRET measurements

Fluorescent images of living cells co-transfected with ECFP, EYFP and HcRed constructs (1 μm thickness) were produced using a Zeiss LSM 510 laser scanning microscope equipped with a Plan-Apochromate 63×, 1.4 oil immersion objective. FRET, if $I_2 - I_1[I_{D2}/I_{D1}] - I_3[I_{A2}/I_{A3}]>0$, where I represents intensities in three channels given in arbitrary units, was determined as described (Baynton et al., 2003). The FRET values were normalized to account for differences in the respective fluorochrome expression levels using the following equation: normalized FRET ($FRET_N$) = FRET/$(I_1 \times I_3)^{1/2}$ according to Xia and Liu (Xia and Liu, 2001). Three color images were taken with three consecutive scans using the following settings: ECFP-RAD54B excitation at λ=458 nm, detection at λ=470-500 nm, EYFP-WRN excitation at λ=488 nm, at λ=500-550 and HcRed-PCNA excitation at λ=543 nm, detection at λ>585 on a Zeiss LSM Meta laser scanning microscope. All co-transfection experiments were repeated at least three times and included an analysis of more than 50 cells.

Antibodies

Anti-WRN mouse monoclonal antibody (Ab) (BD Biosciences Pharmigen, USA), anti WRN polyclonal Ab (ab200 and ab17987), anti-GFP polyclonal (ab290), anti-ATR polyclonal (ab91) and anti-RAD51 monoclonal (ab1839) (Abcam, UK) were used in these studies. Anti-RAD51 (SC H-92), anti-RAD52 (SC H-300), anti-RAD54 (SC H-152), RAD54B (SC N-16), RAD54B (SC K-17), rabbit and goat IgG, and all polyclonal antibodies were obtained from Santa Cruz Biotechnology, Inc. (USA). In addition, anti RAD54 and anti RAD54B rabbit antiserum made against purified Flag-RAD54 and RAD54B proteins were used in the ELISA assay. IgG cross-linking to protein A magnetic beads was done according to New England Biolabs (USA)

Cell extracts, immune-precipitation (IP) and western blot analysis (WB)

Cell pellets were snap frozen in liquid nitrogen before preparing the whole cell lysates. All successive steps were done with ice-cold buffers. Cell pellets were re-suspended in 1× the packed cell volume (PCV) with buffer I (10 mM Tris-HCl, pH 7.8, 100 mM KCl) to which an equal volume of buffer II (10 mM Tris-HCl, pH 8.0, 100 mM KCl, 40% (v/v) glycerol, 0.5% Nonidet P-40, 10 mM EGTA, 10 mM $MgCl_2$, 2 mM DTT, Complete® protease inhibitor, 1 mM PMSF) was added. 1 μl (200 U μl^{-1}) of Omnicleave™ Endonuclease (Epicentre Technologies, WI, USA) was added per 800 μl cell suspension. The cells were briefly sonicated until complete destruction was achieved as determined by microscopy. Total protein concentrations were measured using the Bio-Rad protein assay. Cell extracts were snap frozen in liquid nitrogen and stored in aliquots at –80°C. For each IP, approximately 500 μg of total cell lysate was incubated with the different antibodies covalently linked to protein-A beads, at 4°C over night. The beads were washed 5 times with 0.5 ml buffer mix (1:1) of buffer I: buffer II with 5 mM $MgCl_2$ and 400 U Omnicleave per 50 ml. After washing, the beads were re-suspended in 20 μl NuPAGE™ loading buffer, heated, and loaded on 4-12% Bis-Tris-HCl NuPAGE™ ready gels (Invitrogen) and the separated, immuneprecipitated proteins were subsequently transferred to PVDF membranes (Immobilon™, Millipore). The membranes were blocked (5% dry milk) and the primary rabbit polyclonal or mouse monoclonal antibodies were diluted in dry milk (1%) in PBST (PBS with 0.1% Tween 20). Peroxidase-labeled (HRP) goat anti-rabbit IgG, HRP-horse anti-mouse IgG (Vector Lab, USA), HRP-swine-anti-rabbit IgG or HRP-goat-anti-mouse IgG (DAKO, Denmark) were used as secondary antibodies. Membranes were treated with ECL chemiluminescence reagent (ECL™, Amersham Biosciences) and the bands were visualized by exposing the membranes to Hyperfilm™, ECL™.

Enzyme-linked immunosorbent assays (ELISAs)

All assays were performed in triplicate. Microtiter plates were coated with 1.5 pmol RAD51, WRN or RAD52 diluted in 100 μl PBS at 4° over night. The wells were blocked with 200 μl 2% BSA in 1% Tween 20 in PBS for 2 hours at room temperature (RT). 100 μl of equimolar, two- and fivefold serial dilutions [in 2% BSA, 0.1% Tween20 in PBS (PBST)] of RAD51, RAD52, RAD54, RAD54B or WRN were added to the coated wells and also to wells containing only BSA, and the plates were further incubated for 1 hour at RT. Control wells for antibody specificity and reactivity were included. The wells were then washed five times with 200 μl PBST and thereafter, washed three times with 200 μl PBST between consecutive steps. Primary rabbit antibodies against WRN (ab200 1:1500), RAD51 (SC H92 1:200), RAD52 (SC H300 1:200), RAD54 (rabbit antiserum 1:500), RAD54B (rabbit antiserum 1:3000) and secondary HRP-goat anti rabbit antibody (vector 1:5000) were diluted in PBS and 1 mg ml^{-1} BSA and successively added for 1 hour at RT (100 μl per well). Finally, the substrate (o-phenylenediamine, Dacopatts A/S) was added for 10-30 minutes and stopped with addition of sulfuric acid according to manufacturer's recommendations. Data are presented as mean of duplicates adjusted for background binding to BSA.

Dot blot

500 ng WRN, RAD52, RAD54, RAD54B and BSA were immobilized on a PVDF membrane (Immobilon™, Millipore). The filters were dried, blocked with 5% dry milk in PBS and incubated either with 500 ng ml^{-1} WRN in PBST and 1% dry milk, or with PBST and 1% dry milk alone (to distinguish between specific and unspecific binding of WRN and the antibodies) at 4°C overnight. After washing, the membranes were incubated with the mouse monoclonal anti-WRN (BD, 1:250) in PBST and 1% dry milk at 4°C overnight and developed as an ordinary western blot (see above).

WRN helicase and exonuclease reactions

Reactions (20 or 30 μl) were performed in standard reaction buffer as described previously (Opresko et al., 2002) unless otherwise indicated. DNA substrate concentrations were 2 nM and protein concentrations were as indicated in the figure legends. The reactions were initiated by WRN addition and incubated at 37°C for 15 minutes. To visualize the helicase product, native stop dye was added to the reaction mixture, which was analyzed on a 12% native polyacrylamide gel. Products were visualized by Phosphorimager and were quantitated with ImageQuant Software (Molecular Dynamics). A 12 bp bubble substrate with 19 bp flanking arms (Baynton et al., 2003) and a long fork substrate with a 15 bp fork and 34 bp duplex arm (X/Y substrate) were used as substrates (Opresko et al., 2002).

This work was done partly during the different contributors' stay at the Laboratory of Molecular Gerontology, National Institute on Aging, NIH, USA and partly at Department of Cancer Research and Molecular Medicine, NTNU. We would like to thank Mette Sørensen, Bruno Monterotti and Knut Lauritzen, NTNU, for technical assistance, Ian Hickson, Cancer Research UK Laboratories, Oxford, UK for the generous gift of purified RAD51, and Patrick Sung, Yale University School of Medicine, New Haven, CT, USA for RAD54- and RAD54B-expressing plasmids. We want to thank Patricia Opresko and Wen-Hsing Cheng for critical reading of the manuscript. This work is supported by The Research Council of Norway, The Cancer Fund at St Olav's Hospital, Trondheim, Norway, 2005 Research Fund of University of Ulsan, Korea and Intramural Research Program of the NIH, National Institute on Aging, USA.

References

Aas, P. A., Otterlei, M., Falnes, P. O., Vagbo, C. B., Skorpen, F., Akbari, M., Sundheim, O., Bjoras, M., Slupphaug, G., Seeberg, E. et al. (2003). Human and bacterial oxidative demethylases repair alkylation damage in both RNA and DNA. *Nature* **421**, 859-863.

Akkari, Y. M., Bateman, R. L., Reifsteck, C. A., Olson, S. B. and Grompe, M. (2000). DNA replication is required to elicit cellular responses to psoralen-induced DNA interstrand cross-links. *Mol. Cell. Biol.* **20**, 8283-8289.

Alexeev, A., Mazin, A. and Kowalczykowski, S. C. (2003). Rad54 protein possesses chromatin-remodeling activity stimulated by the Rad51-ssDNA nucleoprotein filament. *Nat. Struct. Biol.* **10**, 182-186.

Barr, S. M., Leung, C. G., Chang, E. E. and Cimprich, K. A. (2003). ATR kinase activity regulates the intranuclear translocation of ATR and RPA following ionizing radiation. *Curr. Biol.* **13**, 1047-1051.

Baynton, K., Otterlei, M., Bjoras, M., von Kobbe, C., Bohr, V. A. and Seeberg, E. (2003). WRN interacts physically and functionally with the recombination mediator protein RAD52. *J. Biol. Chem.* **278**, 36476-36486.

Benson, F. E., Stasiak, A. and West, S. C. (1994). Purification and characterization of the human Rad51 protein, an analogue of *E. coli* RecA. *EMBO J.* **13**, 5764-5771.

Brosh, R. M., Jr, Li, J. L., Kenny, M. K., Karow, J. K., Cooper, M. P., Kureekattil, R. P., Hickson, I. D. and Bohr, V. A. (2000). Replication protein A physically interacts with the Bloom's syndrome protein and stimulates its helicase activity. *J. Biol. Chem.* **275**, 23500-23508.

Brosh, R. M., Jr, Orren, D. K., Nehlin, J. O., Ravn, P. H., Kenny, M. K., Machwe, A. and Bohr, V. A. (1999). Functional and physical interaction between WRN helicase and human replication protein A. *J. Biol. Chem.* **274**, 18341-18350.

Brosh, R. M., Jr, von Kobbe, C., Sommers, J. A., Karmakar, P., Opresko, P. L., Piotrowski, J., Dianova, I., Dianov, G. L. and Bohr, V. A. (2001). Werner syndrome protein interacts with human flap endonuclease 1 and stimulates its cleavage activity. *EMBO J.* **20**, 5791-5801.

Bryan, T. M., Englezou, A., Dalla-Pozza, L., Dunham, M. A. and Reddel, R. R. (1997). Evidence for an alternative mechanism for maintaining telomere length in human tumors and tumor-derived cell lines. *Nat. Med.* **3**, 1271-1274.

Chang, S., Multani, A. S., Cabrera, N. G., Naylor, M. L., Laud, P., Lombard, D., Pathak, S., Guarente, L. and DePinho, R. A. (2004). Essential role of limiting telomeres in the pathogenesis of Werner syndrome. *Nat. Genet.* **36**, 877-882.

Cheng, W. H., Von Kobbe, C., Opresko, P. L., Arthur, L. M., Komatsu, K., Seidman, M. M., Carney, J. P. and Bohr, V. A. (2004). Linkage between werner syndrome protein and the Mre11 complex via Nbs1. *J. Biol. Chem.* **279**, 21169-21176.

Colgin, L. M. and Reddel, R. R. (1999). Telomere maintenance mechanisms and cellular immortalization. *Curr. Opin. Genet. Dev.* **9**, 97-103.

Constantinou, A., Tarsounas, M., Karow, J. K., Brosh, R. M., Bohr, V. A., Hickson, I. D. and West, S. C. (2000). Werner's syndrome protein (WRN) migrates Holliday junctions and co-localizes with RPA upon replication arrest. *EMBO Rep.* **1**, 80-84.

Cooper, M. P., Machwe, A., Orren, D. K., Brosh, R. M., Ramsden, D. and Bohr, V. A. (2000). Ku complex interacts with and stimulates the Werner protein. *Genes Dev.* **14**, 907-912.

Courcelle, J., Donaldson, J. R., Chow, K. H. and Courcelle, C. T. (2003). DNA damage-induced replication fork regression and processing in Escherichia coli. *Science* **299**, 1064-1067.

Cui, S., Arosio, D., Doherty, K. M., Brosh, R. M., Jr, Falaschi, A. and Vindigni, A. (2004). Analysis of the unwinding activity of the dimeric RECQ1 helicase in the presence of human replication protein A. *Nucleic Acids Res.* **32**, 2158-2170.

Cui, S., Klima, R., Ochem, A., Arosio, D., Falaschi, A. and Vindigni, A. (2003). Characterization of the DNA-unwinding activity of human RECQ1, a helicase specifically stimulated by human replication protein A. *J. Biol. Chem.* **278**, 1424-1432.

Davies, S. L., North, P. S., Dart, A., Lakin, N. D. and Hickson, I. D. (2004). Phosphorylation of the Bloom's syndrome helicase and its role in recovery from S-phase arrest. *Mol. Cell. Biol.* **24**, 1279-1291.

De Silva, I. U., McHugh, P. J., Clingen, P. H. and Hartley, J. A. (2000). Defining the

roles of nucleotide excision repair and recombination in the repair of DNA interstrand cross-links in mammalian cells. *Mol. Cell. Biol.* **20**, 7980-7990.

Essers, J., Hendriks, R. W., Swagemakers, S. M., Troelstra, C., de Wit, J., Bootsma, D., Hoeijmakers, J. H. and Kanaar, R. (1997). Disruption of mouse RAD54 reduces ionizing radiation resistance and homologous recombination. *Cell* **89**, 195-204.

Franchitto, A. and Pichierri, P. (2004). Werner syndrome protein and the MRE11 complex are involved in a common pathway of replication fork recovery. *Cell Cycle* **3**, 1331-1339.

Fukuchi, K., Martin, G. M. and Monnat, R. J., Jr (1989). Mutator phenotype of Werner syndrome is characterized by extensive deletions. *Proc. Natl. Acad. Sci. USA* **86**, 5893-5897.

Golub, E. I., Kovalenko, O. V., Gupta, R. C., Ward, D. C. and Radding, C. M. (1997). Interaction of human recombination proteins Rad51 and Rad54. *Nucleic Acids Res.* **25**, 4106-4110.

Grigorova, M., Balajee, A. S. and Natarajan, A. T. (2000). Spontaneous and X-ray-induced chromosomal aberrations in Werner syndrome cells detected by FISH using chromosome-specific painting probes. *Mutagenesis* **15**, 303-310.

Helleday, T. (2003). Pathways for mitotic homologous recombination in mammalian cells. *Mutat. Res.* **532**, 103-115.

Henson, J. D., Neumann, A. A., Yeager, T. R. and Reddel, R. R. (2002). Alternative lengthening of telomeres in mammalian cells. *Oncogene* **21**, 598-610.

Hickson, I. D. (2003). RecQ helicases: caretakers of the genome. *Nat. Rev. Cancer* **3**, 169-178.

Hook, G. J., Kwok, E. and Heddle, J. A. (1984). Sensitivity of Bloom syndrome fibroblasts to mitomycin C. *Mutat. Res.* **131**, 223-230.

Hsu, H. L., Gilley, D., Galande, S. A., Hande, M. P., Allen, B., Kim, S. H., Li, G. C., Campisi, J., Kohwi-Shigematsu, T. and Chen, D. J. (2000). Ku acts in a unique way at the mammalian telomere to prevent end joining. *Genes Dev.* **14**, 2807-2812.

Huang, S., Li, B., Gray, M. D., Oshima, J., Mian, I. S. and Campisi, J. (1998). The premature ageing syndrome protein, WRN, is a 3′→5′ exonuclease. *Nat. Genet.* **20**, 114-116.

Kamath-Loeb, A. S., Johansson, E., Burgers, P. M. and Loeb, L. A. (2000). Functional interaction between the Werner Syndrome protein and DNA polymerase delta. *Proc. Natl. Acad. Sci. USA* **97**, 4603-4608.

Le, S., Moore, J. K., Haber, J. E. and Greider, C. W. (1999). RAD50 and RAD51 define two pathways that collaborate to maintain telomeres in the absence of telomerase. *Genetics* **152**, 143-152.

Lebel, M., Spillare, E. A., Harris, C. C. and Leder, P. (1999). The Werner syndrome gene product co-purifies with the DNA replication complex and interacts with PCNA and topoisomerase I. *J. Biol. Chem.* **274**, 37795-37799.

Leonhardt, H., Rahn, H. P., Weinzierl, P., Sporbert, A., Cremer, T., Zink, D. and Cardoso, M. C. (2000). Dynamics of DNA replication factories in living cells. *J. Cell Biol.* **149**, 271-280.

Lieber, M. R., Ma, Y., Pannicke, U. and Schwarz, K. (2003). Mechanism and regulation of human non-homologous DNA end-joining. *Nat. Rev. Mol. Cell. Biol.* **4**, 712-720.

Lundin, C., Schultz, N., Arnaudeau, C., Mohindra, A., Hansen, L. T. and Helleday, T. (2003). RAD51 is involved in repair of damage associated with DNA replication in mammalian cells. *J. Mol. Biol.* **328**, 521-535.

Martin, G. M. (1978). Genetic syndromes in man with potential relevance to the pathobiology of aging. *Birth. Defects Orig. Artic. Ser.* **14**, 5-39.

Martin, G. M., Sprague, C. A. and Epstein, C. J. (1970). Replicative life-span of cultivated human cells. Effects of donor's age, tissue, and genotype. *Lab. Invest.* **23**, 86-92.

Mazin, A. V., Alexeev, A. A. and Kowalczykowski, S. C. (2003). A novel function of Rad54 protein. Stabilization of the Rad51 nucleoprotein filament. *J. Biol. Chem.* **278**, 14029-14036.

Mosmann, T. (1983). Rapid colorimetric assay for cellular growth and survival: application to proliferation and cytotoxicity assays. *J. Immunol. Methods* **65**, 55-63.

Motycka, T. A., Bessho, T., Post, S. M., Sung, P. and Tomkinson, A. E. (2004). Physical and functional interaction between the XPF/ERCC1 endonuclease and hRad52. *J. Biol. Chem.* **279**, 13634-13639.

Opresko, P. L., Cheng, W. H., von Kobbe, C., Harrigan, J. A. and Bohr, V. A. (2003). Werner syndrome and the function of the Werner protein; what they can teach us about the molecular aging process. *Carcinogenesis* **24**, 791-802.

Opresko, P. L., Laine, J. P., Brosh, R. M., Jr, Seidman, M. M. and Bohr, V. A. (2001). Coordinate action of the helicase and 3′ to 5′ exonuclease of Werner syndrome protein. *J. Biol. Chem.* **276**, 44677-44687.

Opresko, P. L., Otterlei, M., Graakjaer, J., Bruheim, P., Dawut, L., Kolvraa, S., May, A., Seidman, M. M. and Bohr, V. A. (2004). The Werner syndrome helicase and exonuclease cooperate to resolve telomeric D loops in a manner regulated by TRF1 and TRF2. *Mol. Cell* **14**, 763-774.

Opresko, P. L., von Kobbe, C., Laine, J. P., Harrigan, J., Hickson, I. D. and Bohr, V. A. (2002). Telomere-binding protein TRF2 binds to and stimulates the Werner and Bloom syndrome helicases. *J. Biol. Chem.* **277**, 41110-41119.

Otterlei, M., Warbrick, E., Nagelhus, T. A., Haug, T., Slupphaug, G., Akbari, M., Aas, P. A., Steinsbekk, K., Bakke, O. and Krokan, H. E. (1999). Post-replicative base excision repair in replication foci. *EMBO J.* **18**, 3834-3844.

Pichierri, P. and Franchitto, A. (2004). Werner syndrome protein, the MRE11 complex and ATR: menage-a-trois in guarding genome stability during DNA replication? *BioEssays* **26**, 306-313.

Pichierri, P. and Rosselli, F. (2004). The DNA crosslink-induced S-phase checkpoint depends on ATR-CHK1 and ATR-NBS1-FANCD2 pathways. *EMBO J.* **23**, 1178-1187.

Pichierri, P., Rosselli, F. and Franchitto, A. (2003). Werner's syndrome protein is phosphorylated in an ATR/ATM-dependent manner following replication arrest and DNA damage induced during the S phase of the cell cycle. *Oncogene* **22**, 1491-1500.

Rijkers, T., Van Den Ouweland, J., Morolli, B., Rolink, A. G., Baarends, W. M., Van Sloun, P. P., Lohman, P. H. and Pastink, A. (1998). Targeted inactivation of mouse RAD52 reduces homologous recombination but not resistance to ionizing radiation. *Mol. Cell. Biol.* **18**, 6423-6429.

Rosselli, F., Briot, D. and Pichierri, P. (2003). The Fanconi anemia pathway and the DNA interstrand cross-links repair. *Biochimie* **85**, 1175-1184.

Sakamoto, S., Nishikawa, K., Heo, S. J., Goto, M., Furuichi, Y. and Shimamoto, A. (2001). Werner helicase relocates into nuclear foci in response to DNA damaging agents and co-localizes with RPA and Rad51. *Genes Cells* **6**, 421-430.

Salk, D. (1982). Werner's syndrome: a review of recent research with an analysis of connective tissue metabolism, growth control of cultured cells, and chromosomal aberrations. *Hum. Genet.* **62**, 1-5.

Sehorn, M. G., Sigurdsson, S., Bussen, W., Unger, V. M. and Sung, P. (2004). Human meiotic recombinase Dmc1 promotes ATP-dependent homologous DNA strand exchange. *Nature* **429**, 433-437.

Sharma, S., Otterlei, M., Sommers, J. A., Driscoll, H. C., Dianov, G. L., Kao, H. I., Bambara, R. A. and Brosh, R. M., Jr (2004). WRN helicase and FEN-1 form a complex upon replication arrest and together process branch migrating DNA Structures associated with the replication fork. *Mol. Biol. Cell* **15**, 734-750.

Shen, Z., Cloud, K. G., Chen, D. J. and Park, M. S. (1996). Specific interactions between the human RAD51 and RAD52 proteins. *J. Biol. Chem.* **271**, 148-152.

Sigurdsson, S., Van Komen, S., Petukhova, G. and Sung, P. (2002). Homologous DNA pairing by human recombination factors Rad51 and Rad54. *J. Biol. Chem.* **277**, 42790-42794.

Swagemakers, S. M., Essers, J., de Wit, J., Hoeijmakers, J. H. and Kanaar, R. (1998). The human RAD54 recombinational DNA repair protein is a double-stranded DNA-dependent ATPase. *J. Biol. Chem.* **273**, 28292-28297.

Tan, T. L., Kanaar, R. and Wyman, C. (2003). Rad54, a Jack of all trades in homologous recombination. *DNA Repair* **2**, 787-794.

Tanaka, K., Hiramoto, T., Fukuda, T. and Miyagawa, K. (2000). A novel human rad54 homologue, Rad54B, associates with Rad51. *J. Biol. Chem.* **275**, 26316-26321.

Tanaka, K., Kagawa, W., Kinebuchi, T., Kurumizaka, H. and Miyagawa, K. (2002). Human Rad54B is a double-stranded DNA-dependent ATPase and has biochemical properties different from its structural homolog in yeast, Tid1/Rdh54. *Nucleic Acids Res.* **30**, 1346-1353.

Tarsounas, M., Davies, D. and West, S. C. (2003). BRCA2-dependent and independent formation of RAD51 nuclear foci. *Oncogene* **22**, 1115-1123.

Tashiro, S., Kotomura, N., Shinohara, A., Tanaka, K., Ueda, K. and Kamada, N. (1996). S phase specific formation of the human Rad51 protein nuclear foci in lymphocytes. *Oncogene* **12**, 2165-2170.

Teng, S. C. and Zakian, V. A. (1999). Telomere-telomere recombination is an efficient bypass pathway for telomere maintenance in Saccharomyces cerevisiae. *Mol. Cell. Biol.* **19**, 8083-8093.

von Kobbe, C. and Bohr, V. A. (2002). A nucleolar targeting sequence in the Werner syndrome protein resides within residues 949-1092. *J. Cell Sci.* **115**, 3901-3907.

von Kobbe, C., Karmakar, P., Dawut, L., Opresko, P., Zeng, X., Brosh, R. M., Jr, Hickson, I. D. and Bohr, V. A. (2002). Colocalization, physical, and functional interaction between Werner and Bloom syndrome proteins. *J. Biol. Chem.* **277**, 22035-22044.

Wesoly, J., Agarwal, S., Sigurdsson, S., Bussen, W., Van Komen, S., Qin, J., van Steeg, H., van Benthem, J., Wassenaar, E., Baarends, W. M. et al. (2006). Differential contributions of mammalian Rad54 paralogs to recombination, DNA damage repair, and meiosis. *Mol. Cell. Biol.* **26**, 976-989.

West, S. C. (2003). Molecular views of recombination proteins and their control. *Nat. Rev Mol. Cell. Biol.* **4**, 435-445.

Wu, L., Davies, S. L., Levitt, N. C. and Hickson, I. D. (2001). Potential role for the BLM helicase in recombinational repair via a conserved interaction with RAD51. *J. Biol. Chem.* **276**, 19375-19381.

Xia, Z. and Liu, Y. (2001). Reliable and global measurement of fluorescence resonance energy transfer using fluorescence microscopes. *Biophys. J.* **81**, 2395-2402.

Yu, C. E., Oshima, J., Fu, Y. H., Wijsman, E. M., Hisama, F., Alisch, R., Matthews, S., Nakura, J., Miki, T., Ouais, S. et al. (1996). Positional cloning of the Werner's syndrome gene. *Science* **272**, 258-262.

Zhang, N., Kaur, R., Lu, X., Shen, X., Li, L. and Legerski, R. J. (2005). The Pso4 mRNA splicing and DNA repair complex interacts with WRN for processing of DNA interstrand cross-links. *J. Biol. Chem.* **280**, 40559-40567.

Zhang, N., Lu, X. and Legerski, R. J. (2003). Partial reconstitution of human interstrand cross-link repair in vitro: characterization of the roles of RPA and PCNA. *Biochem. Biophys. Res. Commun.* **309**, 71-78.

Zhang, N., Lu, X., Zhang, X., Peterson, C. A. and Legerski, R. J. (2002). hMutSbeta is required for the recognition and uncoupling of psoralen interstrand cross-links in vitro. *Mol. Cell. Biol.* **22**, 2388-2397.

Zheng, H., Wang, X., Warren, A. J., Legerski, R. J., Nairn, R. S., Hamilton, J. W. and Li, L. (2003). Nucleotide excision repair- and polymerase eta-mediated error-prone removal of mitomycin C interstrand cross-links. *Mol. Cell. Biol.* **23**, 754-761.